Current Biology 22, 373–382, March 6, 2012 ©2012 Elsevier Ltd All rights reserved DOI 10.1016/j.cub.2012.01.040

Article

LAR Receptor Tyrosine Phosphatases and HSPGs Guide Peripheral Sensory Axons to the Skin

Fang Wang,[1,*] Sean N. Wolfson,[1] Arash Gharib,[1] and Alvaro Sagasti[1,*]
[1]Department of Molecular, Cell and Developmental Biology, University of California, Los Angeles (UCLA), Los Angeles, CA 90095, USA

Summary

Background: Peripheral axons of somatosensory neurons innervate the skin early in development to detect touch stimuli. Embryological experiments had suggested that the skin produces guidance cues that attract sensory axons, but neither the attractants nor their neuronal receptors had previously been identified.
Results: To investigate peripheral axon navigation to the skin, we combined live imaging of developing zebrafish Rohon-Beard (RB) neurons with molecular loss-of-function manipulations. Simultaneously knocking down two members of the leukocyte antigen-related (LAR) family of receptor tyrosine phosphatases expressed in RB neurons, or inhibiting their function with dominant-negative proteins, misrouted peripheral axons to internal tissues. Time-lapse imaging indicated that peripheral axon guidance, rather than outgrowth or maintenance, was defective in LAR-deficient neurons. Peripheral axons displayed a similar misrouting phenotype in mutants defective in heparan sulfate proteoglycan (HSPG) production and avoided regions in which HSPGs were locally degraded.
Conclusions: HSPGs and LAR family receptors are required for sensory axon guidance to the skin. Together, our results support a model in which peripheral HSPGs are attractive ligands for LAR receptors on RB neurons.

Introduction

The peripheral axons of somatosensory neurons project to the skin early in vertebrate development, allowing animals to sense touch during embryonic stages [1–4]. Little is known about how peripheral sensory axons are guided, but embryological experiments in chick have suggested that axon attractants in the ectoderm play a role: when patches of ectoderm were irradiated or surgically removed, the peripheral axons of dorsal root ganglia (DRG) neurons failed to grow toward the periphery [5, 6]. However, neither the molecular identities of these attractants, nor of the signaling pathways that detect them in somatosensory neurons, have been discovered.

Members of the leukocyte antigen-related (LAR) family of receptor protein tyrosine phosphatases (PTPs) are expressed in DRG neurons of developing mice [7]. The LAR family contains three vertebrate homologs, as well as invertebrate orthologs such as *Drosophila* Dlar and *C. elegans* PTP-3 (reviewed in [8, 9]). Although LAR family proteins play roles in motor and retinal axon guidance, synapse formation, and regeneration of peripheral and central axons (e.g., [10–17]), they have not been implicated in somatosensory neuron development.

*Correspondence: fangwang@ucla.edu (F.W.), sagasti@mcdb.ucla.edu (A.S.)

Biochemical and genetic experiments have demonstrated that heparan sulfate proteoglycans (HSPGs) serve as direct ligands for LAR receptors [18–21]. HSPGs are a diverse group of glycoproteins that, like LAR receptors, have been associated with axon guidance in many types of neurons, including mouse forebrain commissures and retinal axons, zebrafish retinal and motor axons, and ventral midline and motor axons in *Drosophila* and *C. elegans* (e.g., [22–28]). A recent study showed that HSPGs promote axon outgrowth of cultured mouse DRG neurons by clustering PTPσ [21], a LAR family member that regulates axon regeneration [29–33].

Here we describe novel roles for LAR family proteins and HSPGs in the guidance of somatosensory axons to the skin during zebrafish embryogenesis. Reducing expression of two LAR receptors or antagonizing their function with dominant-negative (DN) proteins disrupted innervation of the skin by peripheral sensory axons. Time-lapse imaging suggested that these axons were unable to sense guidance cues that normally steer them to the skin. Peripheral sensory axons in zebrafish deficient in heparan sulfate biosynthesis similarly failed to innervate the skin, and axons avoided regions of skin with lower levels of HSPGs. Together, our results provide a model for the molecular basis of early steps in somatosensory axon guidance.

Results

Three LAR Family Genes Are Expressed in Somatosensory Neurons during Development

Zebrafish trigeminal and Rohon-Beard (RB) neurons project peripheral axons that arborize within the skin between 18 and 36 hr postfertilization (hpf). To identify genes regulating axon morphogenesis, we performed a whole-mount in situ hybridization screen for transmembrane proteins expressed in these neurons at ~24 hpf. Three members of the LAR family of receptor PTPs, *ptprfa*, *ptprfb*, and *ptprdb*, were expressed during development in trigeminal and RB neurons (Figures 1C–1H). Although these genes share expression in somatosensory neurons, they are each expressed in distinct patterns in other tissues. For instance, *ptprfa* is expressed in the ventral spinal cord (likely in motor neurons), *ptprfb* is in the hindbrain and other cranial ganglia, and *ptprdb* is in lateral line neurons and olfactory placodes (Figures 1C–1H; [34, 35]).

Using RT-PCR and rapid amplification of complementary DNA (cDNA) ends (RACE) in 25–28 hpf zebrafish embryos, we identified full-length messenger RNA (mRNA) sequences for the LAR family genes, including alternatively spliced isoforms of PTPRFa (a.1 and a.2) (Figure 1A; see also Figure S1 available online). All these genes contain three Ig domains but include different numbers of FN-III repeats. Phylogenetic comparison of LAR family protein sequences placed PTPRFa and PTPRFb in the same group as mammalian PTPRF proteins and PTPRDb in the PTPRD family (Figure 1B).

PTPRFa and PTPRFb Are Required Redundantly for Somatosensory Axon Innervation of the Skin

To investigate whether LAR receptors function in somatosensory neuron development, we designed two morpholino antisense oligonucleotides for each gene, one targeting a splice

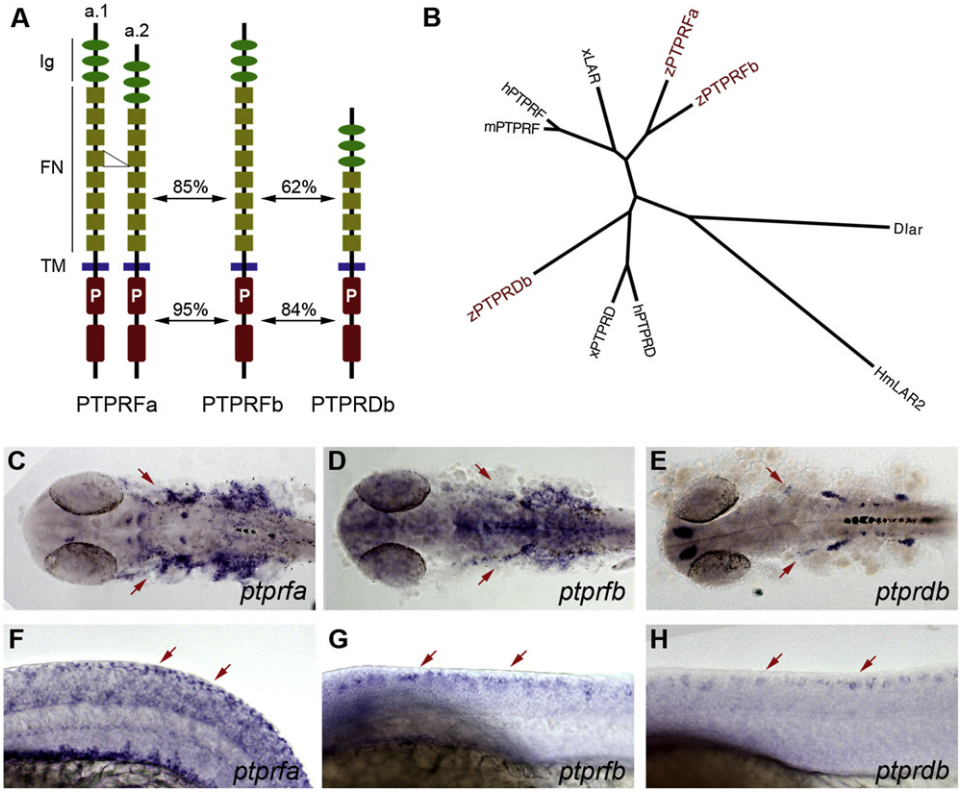

Figure 1. LAR Family Genes Are Expressed in Developing Somatosensory Neurons

(A) Domain structure of zebrafish LAR family proteins. Two alternative splice forms of PTPRFa, differing by one fibronectin III repeat, were identified. Amino acid identities between the ectodomains and cytoplasmic domains separately are indicated. Ig, immunoglobulin-like domain; FN, fibronectin III repeat; TM, transmembrane domain; P, catalytic phosphatase domain.

(B) Phylogenetic relationship between LAR family proteins. Zebrafish PTPRFa and PTPRFb clustered with the PTPRF family, whereas zebrafish PTPRDb was closest to other PTPRD family members. D, fruit fly; Hm, leech; h, human; m, mouse; x, *Xenopus*; z, zebrafish. ClustalW 1.81 was used to compare sequences, and FigTree v1.0 was used to create the tree.

(C–H) Whole-mount in situ hybridization for LAR family members. (C)–(E) show dorsal views, rostral left, 28 hpf; (F)–(H) show lateral views, dorsal up, anterior left; embryo in (F) is 20-somite stage, and embryos in (G) and (H) are 24 hpf. Arrows indicate expression in trigeminal and RB sensory neurons. See also Figure S1.

site (MO1) and the other the translational start site (MO2). RT-PCR verified that MO1 effectively altered splicing, creating truncated mRNAs coding for nonfunctional proteins (Figure S2). These morpholinos were injected into embryos carrying two transgenic reporters—sensory:GFP to visualize somatosensory neurons [36, 37] and krt4:dsRed (*Discosoma* species red fluorescent protein) to visualize the two epithelial layers making up the larval zebrafish skin [38]. To standardize our analysis, we collected confocal images of a 416 square micrometer region of the trunk (Figures 2A–2C; Movie S1) after 48 hpf, when sensory neurons have finished arborizing. This region is innervated by 10–15 RB neurons, representing 5%–8% of all somatosensory neurons. To control for morpholino toxicity, we used a standard control morpholino (Figure 2D).

Ptprdb morpholino knockdown did not obviously disrupt somatosensory neuron morphology (data not shown). Injecting *ptprfa*-MO1 or *ptprfa*-MO2 separately also did not cause a phenotype, but coinjecting the two *ptprfa* morpholinos slightly increased the chance that RB peripheral axons failed to innervate the skin ($p = 0.048$ compared to control) (Figure 2D). Knocking down *ptprfb* (with either morpholino alone or both in combination) caused a similar mild defect in skin innervation ($p = 0.048$–0.092 compared to control) (Figure 2D). Because receptor PTPs often exhibit functional redundancy [39], we hypothesized that coinjecting morpholinos targeting PTPRFa and PTPRFb might generate stronger defects. Indeed, in 78.6% ($n = 28$) of embryos coinjected with *ptprfa*-MO1 and *ptprfb*-MO1, at least one peripheral axon failed to innervate the skin in the trunk region analyzed ($p < 0.001$ compared to control) (Figures 2C and 2D). Coinjecting *ptprfa*-MO2 and *ptprfb*-MO2 disrupted innervation in a similar manner (59.2%, $p < 0.001$). In both cases, double morphant embryos displayed no obvious morphological defects, and RB cell body position and central projections were normal. Some peripheral axons in double morphant embryos projected into internal tissues and wrapped around somites (Figure 2C′; Movie S2), but more often they arborized just below the skin. These observations indicate that PTPRFa and PTPRFb are required in a partially redundant manner for skin innervation by somatosensory neurons.

Dominant-Negative LAR Proteins Disrupt Skin Innervation

To test whether *ptprfa* and *ptprfb* are required cell autonomously for skin innervation, we overexpressed truncated versions of LAR family members in RB neurons. These truncated proteins, comprising the extracellular and transmembrane domains but lacking most of the cytoplasmic domain,

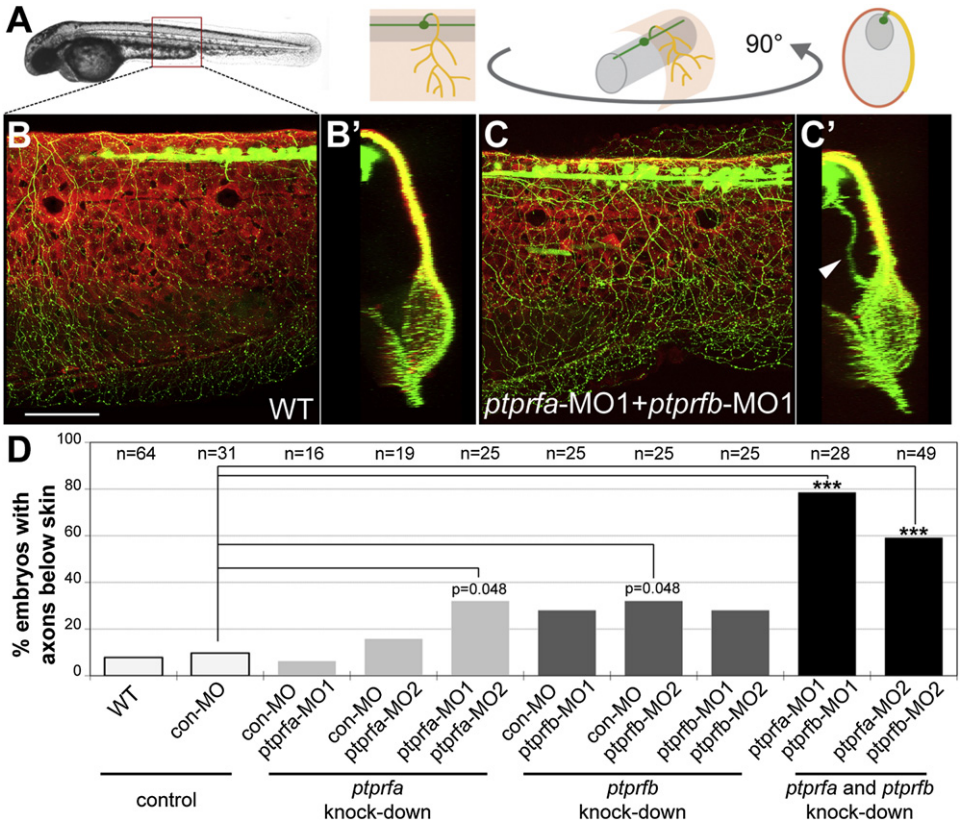

Figure 2. Knocking Down *ptprfa* and *ptprfb* Caused Skin Innervation Defects

(A) Schematic showing the relationship between skin and axons.

(B–C) Confocal projections of lateral views of WT (B) and *ptprfa*/*ptprfb* double morphant (C) embryos. 90° rotations of the images in (B) and (C) provide cross-section views of these embryos (B′–C′). Zebrafish larvae carried two transgenic reporters—sensory:GFP to visualize somatosensory neurons and krt4:dsRed to visualize the skin. Arrowhead indicates axons innervating internal tissues. Scale bar represents 100 μm.

(D) Frequency of embryos with axons below the skin in a defined region of the trunk. Knocking down *ptprfa* or *ptprfb* alone caused mild skin innervation defects compared with embryos injected with an equivalent amount of control morpholino (9.7%). However, axons grew below the skin in 78.6% of *ptprfa*-MO1/*ptprfb*-MO1 double morphants and 59.2% of *ptprfa*-MO2/*ptprfb*-MO2 double morphants, which was significantly ($p < 0.001$) more than controls. Data was analyzed with two-sided Fisher's exact test and computed with R (http://www.r-project.org). See Supplemental Information for details of statistical analysis. Con, control; MO, morphants; ***$p < 0.001$. See also Figure S2 and Movie S1 and S2.

may interfere with LAR function in a DN manner by binding to ligands and preventing them from activating endogenous receptors. We made such putative DN versions of PTPRFb, PTPRDb, and both PTPRFa isoforms. Using a sensory neuron-specific driver and the GAL4/UAS system, each of these putative DN genes, fused to GFP, were expressed by transient transgenesis in single RB neurons of krt4:dsRed transgenic embryos (Figure 3A). All DN receptors were expressed at comparable levels and trafficked to axons (Figure S3).

Skin innervation defects were detected after 48 hpf in 70.4% of RB neurons expressing PTPRFb-DN, 76.9% of neurons expressing PTPRFa.1-DN, and 45.5% of neurons expressing PTPRFa.2-DN (Figures 3B–3H). Like double morphant neurons, some peripheral axons of DN-expressing RB neurons innervated internal tissues (Figure 3E′), whereas others arborized just below the skin (Figure 3H′). In some cases, the entire peripheral arbor of a DN-expressing neuron was underneath the skin (a "severe" defect). Some RB neurons had only one or a few peripheral axon branches below the skin (a "mild" defect) (Figure 3B). In wild-type (WT) animals, the vast majority of RB neurons innervate only the ipsilateral side of the body, but, in some cases, PTPRFa-DN- and PTPRFb-DN-expressing neurons projected axons to both sides of the body (Figure 3D′). Because repulsive interactions between neighboring arbors restrict their territories [37, 40], DN-expressing neurons under the skin may cross to the contralateral side because they do not encounter neighbors. Some trigeminal neurons expressing PTPRFa-DN or PTPRFb-DN also failed to innervate the skin (data not shown), indicating that LAR signaling is required broadly in somatosensory neurons for skin innervation. One out of 13 RB neurons (from ten embryos) overexpressing PTPRDb-DN displayed a mild defect in skin innervation, which did not significantly differ from controls ($p = 0.39$). Overexpressing GFP or putative DN transgenes of two control cell-surface proteins expressed in RB neurons, PTPRN2L and DSCAML, did not cause innervation defects (Figure 3B; data not shown), verifying the specificity of LAR family DN transgenes. These results support the conclusion that PTPRFa and PTPRFb are required redundantly in somatosensory neurons for skin innervation.

LAR family proteins contain two phosphatase-like domains, membrane-proximal D1 and membrane-distal D2, but only D1 is enzymatically active [41]. Phosphatase activity is sometimes dispensable for LAR protein function [42, 43]. To examine whether phosphatase activity is required for skin innervation,

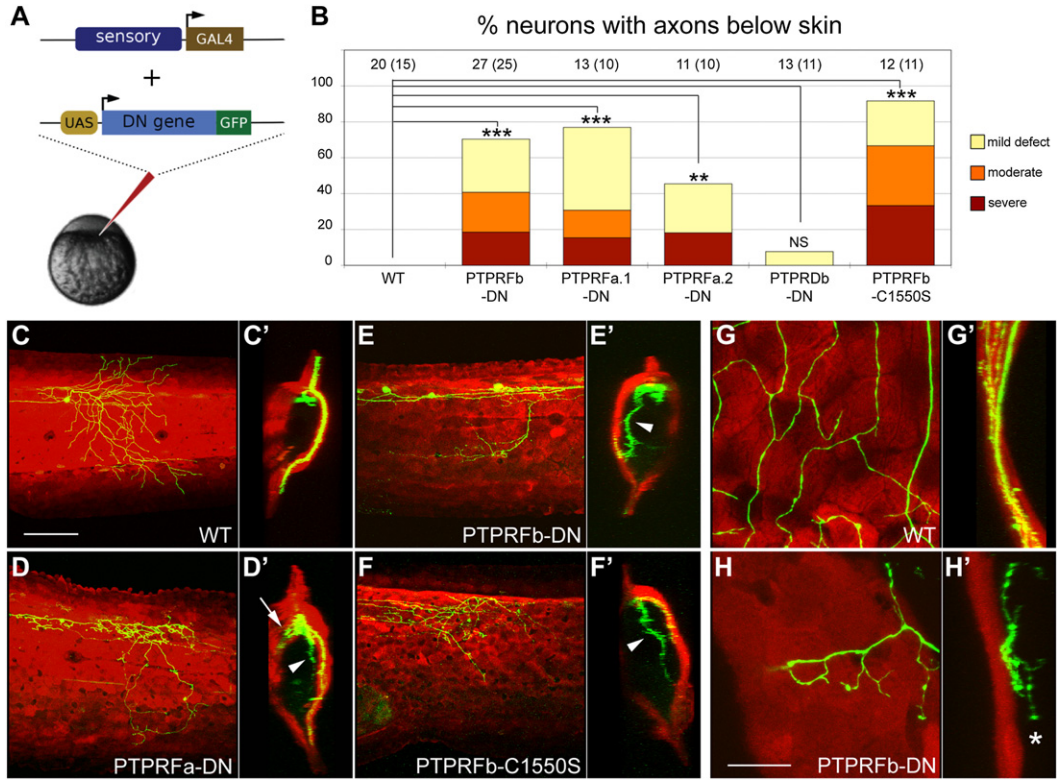

Figure 3. Rohon-Beard Neurons Expressing Dominant-Negative LAR Family Proteins Failed to Innervate Skin

(A) A sensory neuron-specific promoter was used to drive the GAL4-VP16 activator [37]. Putative dominant-negative (DN) versions of each gene, created by replacing their cytoplasmic domains with GFP, were expressed under the control of the Gal4 upstream activation sequence (UAS). Coinjection of these transgenes at the one-cell stage caused transient mosaic expression in somatosensory neurons.

(B) Frequency of RB neurons expressing indicated transgenes with peripheral axons below the skin. Number of neurons are listed at the top of each bar; number of fish in parentheses. Data were analyzed with two-sided Fisher's exact test and computed with R. ***$p < 0.001$; **$p < 0.01$; NS, not significant. Defects were scored as "mild" if one or a few axon branches were below the skin, "moderate" if many axon branches were below the skin, and "severe" if the entire peripheral arbor was below the skin.

(C–F) Confocal projections of lateral views of RB neurons expressing GFP only (WT) (C), PTPRFa.1-DN (D), PTPRFb-DN (E), and PTPRFb-C1550S (F). Ninety degree rotations of the images in (C)–(F) provide cross-section views of embryos (C′–F′), respectively. krt4:dsRed was used to visualize the skin. Arrowheads indicate axons innervating internal tissues; arrow indicates axons innervating the contralateral side of the body. Scale bar represents 100 μm.

(G–H) Higher magnification of lateral view RB neurons expressing GFP only (WT) (G), and PTPRFb-DN (H). Ninety degree rotations are shown in (G′–H′). Star indicates axon arborizing just beneath the skin. Scale bar represents 20 μm. See also Figure S3.

we generated a full-length PTPRFb transgene lacking catalytic activity by mutating a critical cysteine residue in the conserved (I/V)HCXAGXXR(S/T)G sequence of the D1 domain [44] to serine, creating PTPRFb-C1550S. This mutant was fused to GFP and overexpressed in somatosensory neurons using the GAL4/UAS system. Eleven of 12 RB neurons expressing PTPRFb-C1550S displayed skin innervation defects (Figures 3B and 3F′), suggesting that this single amino acid mutation creates a dominant-negative protein and that phosphatase activity is essential for skin innervation. As a control, we overexpressed WT full-length PTPRFb (PTPRFb FL). Most RB neurons overexpressing PTPRFb FL died before 48 hpf, perhaps due to excessive phosphatase activity, but those imaged at earlier stages innervated the skin normally (data not shown). In addition to causing skin innervation defects, PTPRFb-C1550S-expressing neurons also developed aberrant central projection branches, which were never seen in WT neurons and only occasionally seen in neurons expressing PTPRFa-DN or PTPRFb-DN, perhaps suggesting that the phosphatase-dead cytoplasmic domain interferes with the function of intracellular effectors (Figure S3).

PTPRFb-DN-Expressing RB Neurons Display Axon Guidance Defects

Skin innervation defects could result from axon guidance errors, an inability to maintain axonal position or a reduction in the rate of outgrowth that causes axons to miss a developmental window during which the skin can be innervated. To determine how skin innervation goes awry in PTPRFb-DN-expressing neurons, we examined peripheral axon outgrowth in WT and PTPRFb-DN-expressing neurons with in vivo confocal time-lapse imaging. Outgrowth of ascending and descending central projections occurred before peripheral axon outgrowth, as has been described [45]. Around the 18-somite stage (SS), one peripheral axon emerged from the central projection, usually near the cell body. Transient filopodia often initiated from central projections, but only one filopodium persisted, became a growth cone, and grew in a directed manner into the skin (Figures 4A and 4A′; Movie S3). In accordance with the rostral-to-caudal wave of differentiation, rostral RB neurons tended to initiate peripheral axons earlier. RB neurons expressing PTPRFb-DN initiated peripheral axons at the same stages as WT neurons, suggesting that innervation defects

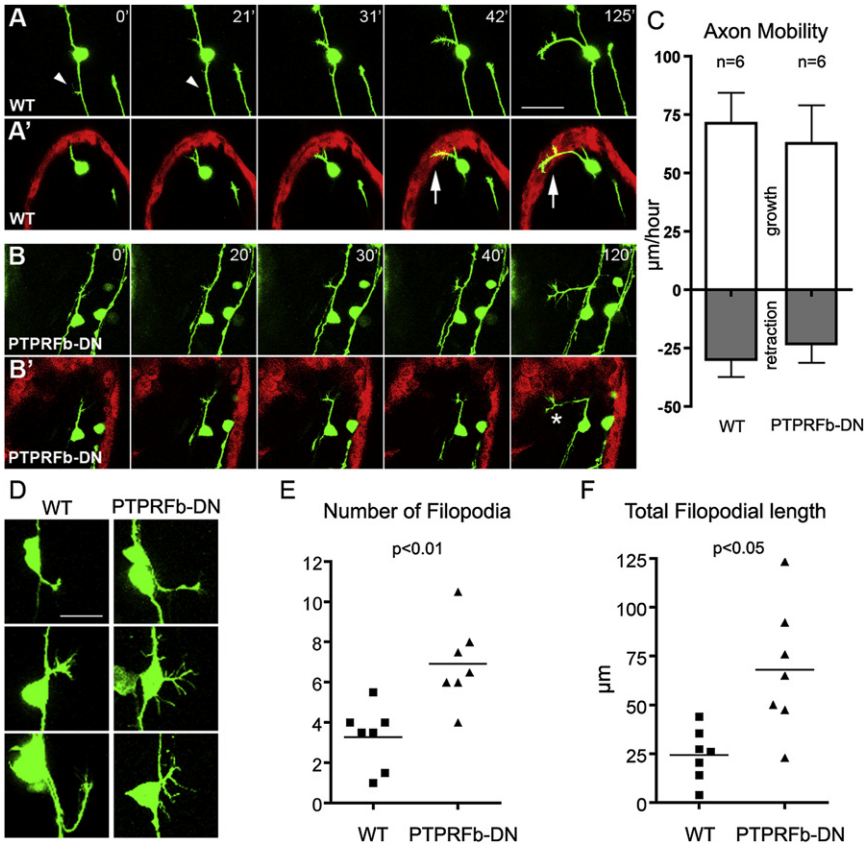

Figure 4. Peripheral Axons of PTPRFb-DN-Expressing RB Neurons Exhibited Axon Guidance Defects at Early Developmental Stages

(A–B) Representative still images from a time-lapse confocal series showing initial peripheral axon outgrowth in WT (A) and PTPRFb-DN-expressing (B) RB neurons. The time-lapse series began at ~18 SS and shows a dorsal view of the embryo. (A) and (B) show projections of complete image stacks of GFP-expressing axons; (A′) and (B′) show 5–7.5 μm optical sections of GFP-expressing axons and dsRed-expressing skin. WT peripheral axons innervated skin (A′), whereas PTPRFb-DN peripheral axons grew just below the skin (B′). Arrows indicate peripheral axon colocalization with keratinocytes. * indicates an axon branching beneath the skin. Arrowheads indicate transient filopodia from the central projection. Scale bar represents 50 μm.

(C) Quantification of axon mobility during initial stages of peripheral axon outgrowth. Peripheral axons of WT and PTPRFb-DN-expressing RB neurons grew and retracted at similar rates. Error bars represent SEM.

(D) Three representative peripheral axons each of WT and PTPRFb-DN-expressing RB neurons. WT axons had not yet reached the skin. Axons of PTPRFb-DN expressing RB neurons had more filopodia and did not enter the skin during the imaging period. Scale bar represents 25 μm.

(E) The peripheral axons of PTPRFb-DN-expressing RB neurons had significantly ($p < 0.01$) more filopodia than axons of WT neurons.

(F) The total filopodial length of axons in PTPRFb-DN expressing RB neurons was significantly ($p < 0.05$) longer than in WT axons. All data were analyzed with two-tailed t test. See also Movie S3 and S4.

were not due to delayed outgrowth. WT peripheral axons entered the skin on average 89 min after initiation (n = 10). Fourteen of 15 axons in PTPRFb-DN-expressing neurons did not innervate the skin during the imaging period (2–4 hr after peripheral axon initiation) but instead grew below it (Figures 4B and 4B′; Movie S4). WT axons never branched before entering the skin, but seven of the 15 PTPRFb-DN-expressing neurons began branching below the skin during the observation period (Figure 4B′).

To further analyze peripheral axon pathfinding behavior, we traced the trajectories of WT and PTPRFb-DN-expressing neurons in three dimensions for the first hour after initiation. Only axons that had not yet entered the skin were analyzed, ensuring that the axons of WT and PTPRFb-DN-expressing neurons were in comparable environments. Axons of WT and PTPRFb-DN-expressing RB neurons grew and retracted at similar rates (Figure 4C). Axons of PTPRFb-DN-expressing neurons did not pause beneath the skin nor did they appear to make failed attempts to enter it (Movie S4). However, when peripheral axons were below the skin, PTPRFb-DN-expressing RB neurons had more elaborate filopodia than WT axons. To characterize this phenotype, we evaluated WT axon morphology just before they entered the skin (from 32 to 185 min after axon initiation) and the morphology of axons in PTPRFb-DN-expressing neurons between 80 and 100 min after axon initiation. Peripheral axons of PTPRFb-DN-expressing neurons had significantly more filopodia than WT axons (Figures 4D–4F). In contrast to all WT axons, some axons of PTPRFb-DN-expressing neurons lacked a clear leading growth cone (Figure 4D), suggesting that they failed to perceive directional cues. Together these time-lapse imaging studies suggest that expression of PTPRFb-DN disrupts axon guidance, rather than maintenance or timing of outgrowth.

Proteoglycan Binding Sites on LAR Proteins Contribute to Skin Innervation

HSPGs and chondroitin sulfate proteoglycans (CSPGs) bind to the first Ig domain of LAR receptors [20, 21, 30]. To test whether proteoglycan binding is involved in skin innervation, we deleted the first Ig domain (Ig1) in the PTPRFb-DN transgene (PTPRFb-DN ΔIG1). Although PTPRFb-DN ΔIG1 was expressed in axons at levels comparable to the unmutated PTPRFb-DN, as judged by GFP expression (Figure S3), it caused significantly fewer innervation defects (11.8% versus 70.4%). We next created mutations in the Ig1 domain of the PTPRFb-DN ectodomain that compromise proteoglycan binding. Two conserved motifs, KKGKK and RTHR, are important for LAR receptor recognition of HSPGs [20]; KKGKK is also required for recognizing CSPGs [30]. We separately mutated these two sequences to AAGAA and ATHA, respectively, in the PTPRFb-DN transgene, generating PTPRFb-DN mutant 1 (Mu1) and PTPRFb-DN mutant 2 (Mu2). Expressing PTPRFb-DN Mu1 in RB neurons caused significantly fewer and milder skin innervation defects than the unmutated PTPRFb-DN transgene (Figure 5A), indicating that Mu1 was compromised in its ability to compete with endogenous LAR receptors for ligands. Mu2 (ATHA) did not reduce defects

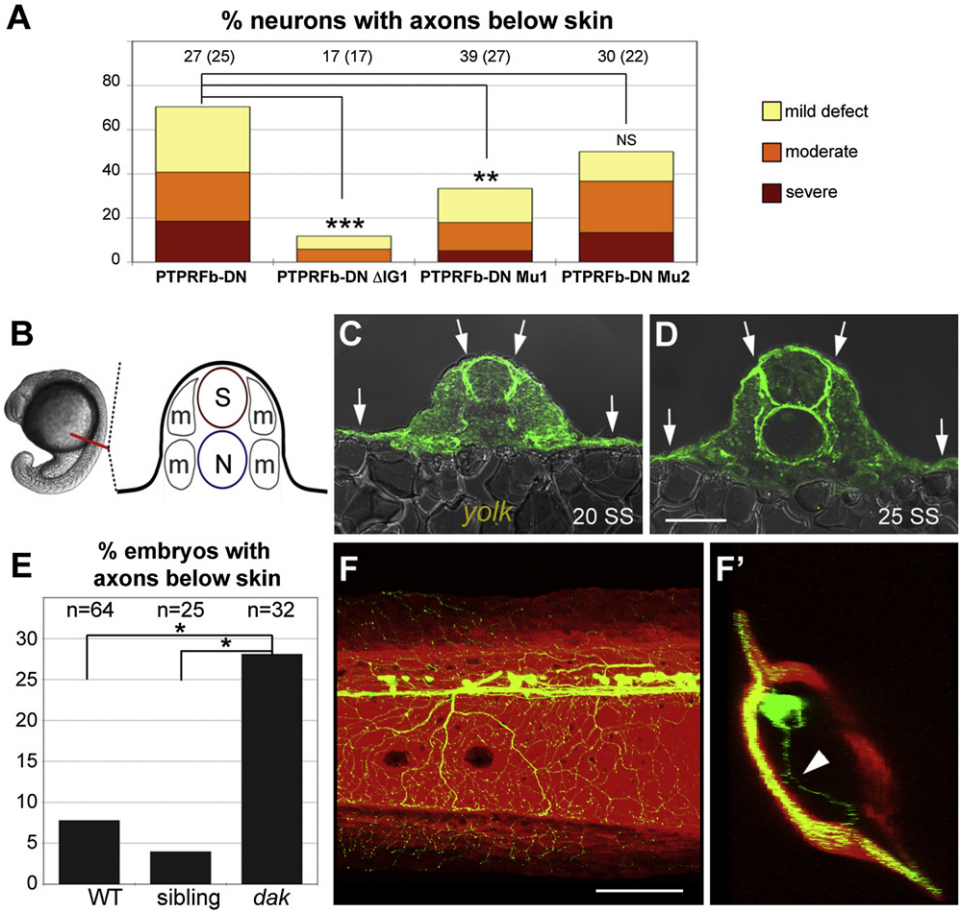

Figure 5. HSPG Binding to LAR Proteins Is Likely Important for Skin Innervation

(A) Disrupting the first Ig domain significantly reduced skin innervation defects caused by expressing PTPRFb-DN. Deleting Ig1 or mutating a proteoglycan-binding-site (Mu1) in PTPRFb-DN significantly reduced skin innervation defects (11.8% and 33.3%, respectively). The number of neurons is listed at the top of each bar; the number of fish is listed in parenthesis.

(B) Diagram of ~20 SS zebrafish embryo cross-section. Red line indicates position of cross-section. S, spinal cord; N, notochord; m, muscle.

(C and D) Cross-sections of anti-HS staining at 20 and 25 SS. HSPGs were enriched in basement membranes around the spinal cord, notochord, and skin. Arrows indicate high levels of anti-HS staining in the skin. Scale bar represents 50 μm.

(E) Frequency of embryos with peripheral axons below the skin in a defined region of the trunk (see Figure 2). Peripheral axons in this region were found below the skin in 28.1% of *dackel* homozygous mutant embryos, which was significantly higher than in their nonmutant siblings (4.0%).

(F) Lateral view of 3 dpf *dackel* mutant larva harboring krt4:dsRed and sensory:GFP transgenes.

(F′) Ninety degree rotation of image in (F). Arrowhead indicates axon innervating internal tissue. All data analyzed with two-sided Fisher's exact test and computed with R. ***$p < 0.001$; **$p < 0.01$; *$p < 0.05$. Scale bar represents 100 μm. See also Figure S4.

significantly, perhaps indicating that this region is less important for proteoglycan binding in vivo.

HSPGs Are Required for Skin Innervation

To examine HSPG expression, we stained 20 and 25 SS embryos with an antibody recognizing heparan sulfate (HS) and imaged embryos in cross-section. HS staining was found throughout the embryo at these stages but was enriched in basement membranes, including the basement membrane of the skin (Figures 5B–5D). To test whether HSPGs influence skin innervation, we crossed our skin and sensory neuron transgenic reporters to *dackel* mutants, which harbor a lesion in the gene encoding the EXT2 glycosyltransferase, an enzyme required for heparan sulfate synthesis [25]. Skin innervation defects in the analyzed trunk region, similar to those in *ptprfa*/*ptprfb* double morphants, were detected in 28% (n = 32) of *dackel* mutants imaged after 48 hpf. In contrast, only 4% (n = 25) of nonmutant siblings (including WT and heterozygous animals) displayed a skin innervation defect (Figures 5E, 5F, and 5F′). As has been suggested for other phenotypes [25], the modest penetrance of skin innervation defects in *dackel* mutants is likely due to rescue by maternally provided EXT2, because HS staining was similar in WT and *dackel* mutants at 18–20 SS but completely absent from skin in 3 dpf *dackel* mutants (Figure S4).

HSPGs Are Likely Attractants for Peripheral Sensory Axons

HSPGs and LAR family proteins may act permissively, to allow axons to enter the skin, or instructively, in attractive or repellent pathways that guide axons. To distinguish between these possibilities, we injected heparinase III, an enzyme that specifically degrades heparan sulfate, locally (near the end of yolk extension) into embryos at approximately 16 SS, before peripheral axon arborization. If HSPGs act permissively, peripheral axons should simply fail to innervate the skin in

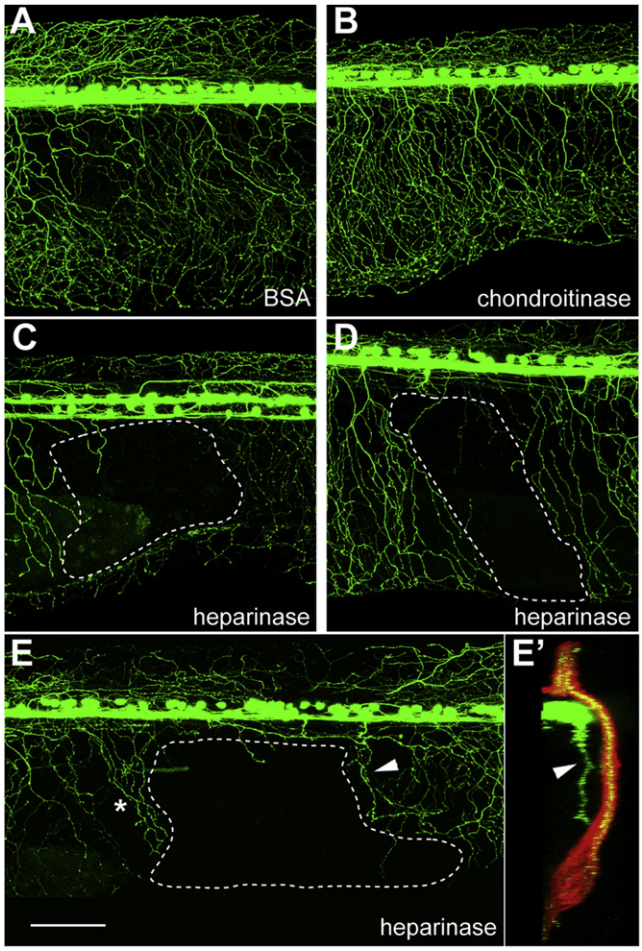

Figure 6. Peripheral Axons Avoid Heparinase III-Injected Areas

(A–E) Lateral views of 2 dpf embryos injected with BSA (A) or chondroitinase ABC (B). These embryos did not exhibit obvious defects in RB neuron projections. However, RB neuron peripheral axons often did not innervate heparinase III-injected areas (C–E), suggesting that peripheral axons prefer regions with higher levels of heparan sulfate.

(E′) A 90° rotation of (E). Arrowheads in (E) and (E′) indicate an axon that innervated internal tissue. * indicates another axon with a branches beneath the skin. White dotted lines indicate under-innervated areas. Scale bar represented 100 μm. See also Figure S5 and Movies S5 and S6.

heparinase III-injected areas; if HSPGs are attractants, peripheral axons should avoid heparinase III-injected areas, because higher levels of attractants would be present outside of them; if HSPGs are repellents, peripheral axons should be attracted to heparinase III-injected areas. Injecting bovine serum albumin (BSA) or chondroitinase ABC, an enzyme that degrades chondroitin sulfate and chondroitin, did not alter skin innervation (Figures 6A and 6B) but many heparinase III-injected embryos contained regions devoid of innervation (Figures 6C–6E). These under-innervated areas were always near the end of the yolk extension, where heparinase III was injected, suggesting that axons avoided these areas. The number of RB neurons was similar to controls near the heparinase III-injected areas, indicating that heparinase III did not cause excessive cell death. Occasionally, a few axons projected near the under-innervated area, but these axons often arborized below the skin (Figures 6E and E′).

To determine whether lack of innervation of a skin region deficient in HSPGs is caused by local axon degeneration, retraction away from these areas, or a guidance defect, we made time-lapse movies of heparinase-injected embryos and compared them to movies of embryos injected with BSA. These analyses revealed that axons did not first grow into these regions and then retract or degenerate (n = 5). Rather, at stages when RB axons in control embryos steadily grew ventrally, RB axons near heparinase-injected regions either turned away from these regions, branched upon encountering them, or grew at a reduced rate compared to their neighbors (which can be a characteristic of axons lacking guidance cues [46]) (Figure S5; Movies S5 and S6). Together, these experiments favor the model that HSPGs are attractants for peripheral sensory axons and that reducing them locally leads to reduced innervation relative to adjacent skin regions.

PTPRFb May Act in a Pathway with HSPGs in Skin Innervation

To test further whether LAR proteins are receptors for HSPGs, we combined manipulations that compromised LAR and HSPG function. Injecting *ptprfa* or *ptprfb* morpholinos alone did not dramatically affect RB peripheral axons, and *dackel* mutants alone displayed mild skin innervation defects. However, injecting *ptprfb*-MO1 or *ptprfb*-MO2 into *dackel* mutants substantially increased the frequency of embryos with axons below the skin in the analyzed trunk region (Figure 7). In contrast, injecting *ptprfa*-MO1, or *ptprfa*-MO1 and *ptprfa*-MO2 together, did not enhance skin innervation defects of *dackel* mutants (Figure 7). One explanation for these results is that PTPRFb is the primary receptor for HSPGs during skin innervation. Surprisingly, injecting both *ptprfa* and *ptprfb* morpholinos together into *dackel* mutants did not further enhance this phenotype. *dackel* mutant embryos injected with morpholinos targeting both genes were noticeably sick and many died before 3 dpf, so perhaps only mildly affected embryos survived to 48 hpf. Nonetheless, together with our finding that mutating HSPG binding sites in the PTPRFb-DN transgene reduced its potency, the robust synergy between *ptprfb* morpholinos and *dackel* mutants is consistent with PTPRFb acting in a pathway with HSPGs to guide axons to the skin.

Discussion

Innervation of the skin by the peripheral axons of somatosensory neurons is a key step in the development of somatosensory circuits. Although embryological experiments in chick had suggested that peripheral axons are guided by attractants in the skin [5, 6], neither the molecular nature of the attractants nor their receptors had been identified. By combining loss-of-function manipulations with live imaging of peripheral axons in zebrafish, we have implicated LAR receptors and HSPGs in guiding these axons, demonstrating new roles for these protein families.

LAR family members play roles in guiding retinal and motor axons in both vertebrates and invertebrates (reviewed in [9]) but had not previously been implicated in the guidance of cutaneous somatosensory axons. Several lines of evidence support the conclusion that LAR family receptors function in peripheral axon guidance: (1) knocking down two LAR family proteins (PTPRFa and PTPRFb) with morpholinos caused the frequent misrouting of peripheral axons, (2) sensory neuron-specific overexpression of truncated versions of PTPRFa or PTPRFb caused similar defects, and (3) time-lapse imaging

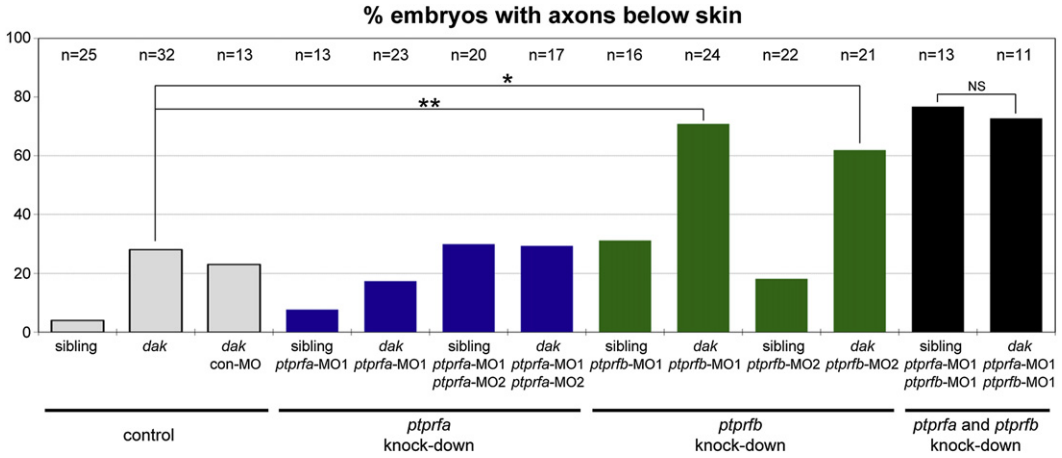

Figure 7. PTPRFb and HSPGs Likely Function in the Same Pathway

Injecting *ptprfb*-MO1 or *ptprfb*-MO2 into *dackel* mutants significantly increased the frequency (70.8% and 61.9%, respectively) of embryos with axons below the skin in a defined area of the trunk (see Figure 2), but *ptprfa*-MO1 or *ptprfa*-MO1 and *ptprfa*-MO2 together did not cause similar synergistic effects. Skin innervation defects were displayed in this region in 72.7% of *dackel* mutants injected with *ptprfa*-MO1/*ptprfb*-MO1 morpholinos, which is not significantly different from nonmutant siblings injected with both morpholinos. Data were analyzed with two-sided Fisher's exact test and computed with R. $^{**}p < 0.01$; $^{*}p < 0.05$.

revealed that axons expressing these truncated proteins have less polarized growth cones and fail to innervate skin from early stages of outgrowth. The fact that LAR family receptors are also expressed in developing mouse somatosensory neurons suggests that their roles in cutaneous guidance are conserved [7].

The finding that innervation defects caused by morpholino knockdown were less penetrant than those caused by DN proteins (5%–10% of neurons in double morphants versus 45%–80% in dominant-negative-expressing neurons) suggests that yet another LAR family protein may contribute to skin innervation. This protein is unlikely to be PTPRFDb, because overexpressing a truncated version of this gene caused few innervation defects. We also found stronger defects when we imaged initial axon outgrowth (>90% under the skin) than when we imaged axons at 54 hpf (45%–80% at least partially under the skin). This implies that some misprojecting RB neurons died between 18 and 54 hpf, perhaps from a deficiency in neurotrophic or mechanical support. Misprojecting axons that do survive to 54 hpf often followed the trajectories of motor or lateral line axons, suggesting that they may interact with the Schwann cells associated with those neurons. This is an intriguing possibility, because in the absence of Schwann cells, lateral line axons associate with the skin [47]. Thus, lateral line and RB neurons may both have the potential to interact with skin or Schwann cells, but each display a preference for one over the other. LAR signaling thus endows RB neurons with the ability to make the appropriate choice between two potentially supportive tissue environments.

Several experiments supported the hypothesis that HSPGs are attractive ligands that activate LAR signaling in growth cones: (1) mutating a proteoglycan binding site in LAR DN transgenes reduced their dominant-negative effect, (2) RB axons often failed to target the skin in *dackel* mutants, which are defective in the synthesis of heparan sulfate [25], and (3) axons avoided regions of skin injected with heparinase III, an enzyme that degrades heparan sulfate. Staining for HSPGs indicated that they are located in many parts of the zebrafish embryo, raising the question of how they could guide peripheral axons specifically to a particular tissue. Because LAR proteins may have different affinities for specific HSPGs, it is possible that a particular proteoglycan is most attractive to peripheral sensory axons and is produced specifically in the skin. Intriguingly, we found that although the ectodomain of PTPRFb potently disrupts peripheral axon guidance, the ectodomain of its relative PTPRDb does not. It is possible that the PTPRDb Ig1 domain does not bind to proteoglycans at all or, more intriguingly, that the Ig1 domains of the two proteins have different affinities for particular proteoglycans.

HSPGs are often thought not to act as signals themselves, but rather as factors that modify the availability of other signaling proteins. For example, HSPGs regulate FGF signaling to control guidance of retinal axons in *Xenopus* [48] and modify Slit/Robo signaling to influence guidance of zebrafish retinal axons [25]. It is possible that HSPG/LAR signaling in somatosensory neurons similarly modifies the function of another pathway to regulate guidance of peripheral sensory neurons. However, the most parsimonious explanation for the striking similarity between defects in LAR deficient embryos and *dackel* mutants, as well as the fact that proteoglycan binding sites are required in truncated LAR proteins for their dominant-negative effects, is that HSPGs are direct attractive ligands for LAR receptors on growth cones. A recent study found that HSPGs can directly promote outgrowth of DRG neurons in culture by clustering LAR family receptors [21], providing a mechanistic explanation for how HSPGs may guide axons to the skin.

Experimental Procedures

Embryos

Zebrafish embryos were raised at 28.5°C. Because *dackel* mutants (gift of Chi-Bin Chien) are homozygous lethal, heterogygous *dackel* fish were crossed to Tg(sensory:GFP) and Tg(krt4:dsRed) lines [38]. *dackel*/+ progeny were incrossed to produce homozygous *dackel* embryos with both GFP and dsRed labeling. Animal care and experimental procedures were approved by the UCLA Chancellor's Animal Research Committee.

In Situ Hybridization and Immunostaining

In situ hybridization was performed according to the Thisse Lab In Situ Hybridization Protocol 2010 Update (https://wiki.zfin.org/display/prot/Thisse+Lab+-+In+Situ+Hybridization+Protocol+-+2010+update). Details of

probe design are available in the Supplemental Information. Immunocytochemistry was performed on cryosectioned tissue with an anti-heparan sulfate primary antibody (10E4, Seikagaku Biobusiness Corporation and United States Biological) at 1:100 and an anti-mouse Alexa 488 secondary antibody (Invitrogen) at 1:500.

Morpholino Injection

Morpholinos were injected into one-cell stage embryos. The efficacy of splice blocking morpholinos was verified by RT-PCR. Details of morpholino design, RT-PCR primer sequences, and concentrations used for injections are available in the Supplemental Information.

Time-Lapse Imaging and Image Analysis

Mounting and time-lapse imaging were performed as previously described [49]. NeuroLucida software (Microbrightfield, Williston, VT) was used to generate three-dimensional tracings of peripheral axons from confocal stacks for quantification. Details of quantification methods are described in the Supplemental Information.

Cloning and Transgene Construction

The Tol2/Gateway zebrafish kit developed by the laboratory of Chi-Bin Chien was used for construction of most plasmids [50]. The full-length sequences for ptprfa.1, ptprfa.2, and ptprdb were deposited in GenBank (see Accession Numbers). PCR was used to amplify PTPRFa.1-DN, PTPRFa.2-DN, and PTPRDb-DN from 25–28 hpf zebrafish cDNA and PTPRFb-DN, PTPRFb-full length from a cDNA clone (clone id: 8003994, Open Biosystem). Sequences are shown in Figure S1. Details of cloning methods are provided in the Supplemental Information.

Heparinase Injections

16-somite embryos were dechorionated and embedded in 1% low-melting-point agarose in Ringer's solution. Chondroitinase ABC (Sigma) and heparinase III (Sigma) were dissolved to 1 mg/ml and 1 U/ml, respectively. For each fish, ~5 nl of these solutions were injected under the skin near the yolk extension. BSA (1mg/ml) was injected as a control.

Accession Numbers

The full-length sequences for ptprfa.1, ptprfa.2, and ptprdb were deposited in GenBank under accession numbers JQ414007, JQ414008, and JQ414009, respectively.

Supplemental Information

Supplemental Information includes five figures, Supplemental Experimental Procedures, and six movies and can be found with this article online at doi:10.1016/j.cub.2012.01.040.

Acknowledgments

We thank Shawn J. Cokus for assistance with statistics, Lok Kwan Leung for help with the in situ hybridization screen, and Majid Husain for generating the krt4:dsRed transgenic line. We also thank Larry Zipursky, Bill Lowry, and members of the Sagasti laboratory for critical comments on the manuscript. This work was supported by awards from the Esther A. and Joseph Klingenstein Fund, the Whitehall Foundation, the Burroughs Wellcome Fund, and a grant from the National Institute of Dental and Craniofacial Research.

Received: September 16, 2011
Revised: January 6, 2012
Accepted: January 20, 2012
Published online: February 9, 2012

References

1. Moore, S.J., and Munger, B.L. (1989). The early ontogeny of the afferent nerves and papillary ridges in human digital glabrous skin. Brain Res. Dev. Brain Res. *48*, 119–141.
2. Davies, A., and Lumsden, A. (1984). Relation of target encounter and neuronal death to nerve growth factor responsiveness in the developing mouse trigeminal ganglion. J. Comp. Neurol. *223*, 124–137.
3. Metcalfe, W.K., Myers, P.Z., Trevarrow, B., Bass, M.B., and Kimmel, C.B. (1990). Primary neurons that express the L2/HNK-1 carbohydrate during early development in the zebrafish. Development *110*, 491–504.
4. Saint-Amant, L., and Drapeau, P. (1998). Time course of the development of motor behaviors in the zebrafish embryo. J. Neurobiol. *37*, 622–632.
5. Honig, M.G., Camilli, S.J., and Xue, Q.S. (2004). Ectoderm removal prevents cutaneous nerve formation and perturbs sensory axon growth in the chick hindlimb. Dev. Biol. *266*, 27–42.
6. Martin, P., Khan, A., and Lewis, J. (1989). Cutaneous nerves of the embryonic chick wing do not develop in regions denuded of ectoderm. Development *106*, 335–346.
7. Schaapveld, R.Q., Schepens, J.T., Bächner, D., Attema, J., Wieringa, B., Jap, P.H., and Hendriks, W.J. (1998). Developmental expression of the cell adhesion molecule-like protein tyrosine phosphatases LAR, RPTPdelta and RPTPsigma in the mouse. Mech. Dev. *77*, 59–62.
8. Chagnon, M.J., Uetani, N., and Tremblay, M.L. (2004). Functional significance of the LAR receptor protein tyrosine phosphatase family in development and diseases. Biochem. Cell Biol. *82*, 664–675.
9. Johnson, K.G., and Van Vactor, D. (2003). Receptor protein tyrosine phosphatases in nervous system development. Physiol. Rev. *83*, 1–24.
10. Desai, C.J., Gindhart, J.G., Jr., Goldstein, L.S., and Zinn, K. (1996). Receptor tyrosine phosphatases are required for motor axon guidance in the Drosophila embryo. Cell *84*, 599–609.
11. Krueger, N.X., Van Vactor, D., Wan, H.I., Gelbart, W.M., Goodman, C.S., and Saito, H. (1996). The transmembrane tyrosine phosphatase DLAR controls motor axon guidance in Drosophila. Cell *84*, 611–622.
12. Stepanek, L., Stoker, A.W., Stoeckli, E., and Bixby, J.L. (2005). Receptor tyrosine phosphatases guide vertebrate motor axons during development. J. Neurosci. *25*, 3813–3823.
13. Clandinin, T.R., Lee, C.H., Herman, T., Lee, R.C., Yang, A.Y., Ovasapyan, S., and Zipursky, S.L. (2001). Drosophila LAR regulates R1-R6 and R7 target specificity in the visual system. Neuron *32*, 237–248.
14. Maurel-Zaffran, C., Suzuki, T., Gahmon, G., Treisman, J.E., and Dickson, B.J. (2001). Cell-autonomous and -nonautonomous functions of LAR in R7 photoreceptor axon targeting. Neuron *32*, 225–235.
15. Rashid-Doubell, F., McKinnell, I., Aricescu, A.R., Sajnani, G., and Stoker, A. (2002). Chick PTPsigma regulates the targeting of retinal axons within the optic tectum. J. Neurosci. *22*, 5024–5033.
16. Van der Zee, C.E., Man, T.Y., Van Lieshout, E.M., Van der Heijden, I., Van Bree, M., and Hendriks, W.J. (2003). Delayed peripheral nerve regeneration and central nervous system collateral sprouting in leucocyte common antigen-related protein tyrosine phosphatase-deficient mice. Eur. J. Neurosci. *17*, 991–1005.
17. Xie, Y., Yeo, T.T., Zhang, C., Yang, T., Tisi, M.A., Massa, S.M., and Longo, F.M. (2001). The leukocyte common antigen-related protein tyrosine phosphatase receptor regulates regenerative neurite outgrowth in vivo. J. Neurosci. *21*, 5130–5138.
18. Fox, A.N., and Zinn, K. (2005). The heparan sulfate proteoglycan syndecan is an in vivo ligand for the Drosophila LAR receptor tyrosine phosphatase. Curr. Biol. *15*, 1701–1711.
19. Johnson, K.G., Tenney, A.P., Ghose, A., Duckworth, A.M., Higashi, M.E., Parfitt, K., Marcu, O., Heslip, T.R., Marsh, J.L., Schwarz, T.L., et al. (2006). The HSPGs Syndecan and Dallylike bind the receptor phosphatase LAR and exert distinct effects on synaptic development. Neuron *49*, 517–531.
20. Aricescu, A.R., McKinnell, I.W., Halfter, W., and Stoker, A.W. (2002). Heparan sulfate proteoglycans are ligands for receptor protein tyrosine phosphatase sigma. Mol. Cell. Biol. *22*, 1881–1892.
21. Coles, C.H., Shen, Y., Tenney, A.P., Siebold, C., Sutton, G.C., Lu, W., Gallagher, J.T., Jones, E.Y., Flanagan, J.G., and Aricescu, A.R. (2011). Proteoglycan-specific molecular switch for RPTPσ clustering and neuronal extension. Science *332*, 484–488.
22. Bülow, H.E., and Hobert, O. (2004). Differential sulfations and epimerization define heparan sulfate specificity in nervous system development. Neuron *41*, 723–736.
23. Inatani, M., Irie, F., Plump, A.S., Tessier-Lavigne, M., and Yamaguchi, Y. (2003). Mammalian brain morphogenesis and midline axon guidance require heparan sulfate. Science *302*, 1044–1046.
24. Johnson, K.G., Ghose, A., Epstein, E., Lincecum, J., O'Connor, M.B., and Van Vactor, D. (2004). Axonal heparan sulfate proteoglycans regulate the distribution and efficiency of the repellent slit during midline axon guidance. Curr. Biol. *14*, 499–504.

25. Lee, J.S., von der Hardt, S., Rusch, M.A., Stringer, S.E., Stickney, H.L., Talbot, W.S., Geisler, R., Nüsslein-Volhard, C., Selleck, S.B., Chien, C.B., and Roehl, H. (2004). Axon sorting in the optic tract requires HSPG synthesis by ext2 (dackel) and extl3 (boxer). Neuron *44*, 947–960.
26. Steigemann, P., Molitor, A., Fellert, S., Jäckle, H., and Vorbrüggen, G. (2004). Heparan sulfate proteoglycan syndecan promotes axonal and myotube guidance by slit/robo signaling. Curr. Biol. *14*, 225–230.
27. Schneider, V.A., and Granato, M. (2006). The myotomal diwanka (lh3) glycosyltransferase and type XVIII collagen are critical for motor growth cone migration. Neuron *50*, 683–695.
28. Xiao, T., and Baier, H. (2007). Lamina-specific axonal projections in the zebrafish tectum require the type IV collagen Dragnet. Nat. Neurosci. *10*, 1529–1537.
29. McLean, J., Batt, J., Doering, L.C., Rotin, D., and Bain, J.R. (2002). Enhanced rate of nerve regeneration and directional errors after sciatic nerve injury in receptor protein tyrosine phosphatase sigma knock-out mice. J. Neurosci. *22*, 5481–5491.
30. Shen, Y., Tenney, A.P., Busch, S.A., Horn, K.P., Cuascut, F.X., Liu, K., He, Z., Silver, J., and Flanagan, J.G. (2009). PTPsigma is a receptor for chondroitin sulfate proteoglycan, an inhibitor of neural regeneration. Science *326*, 592–596.
31. Sapieha, P.S., Duplan, L., Uetani, N., Joly, S., Tremblay, M.L., Kennedy, T.E., and Di Polo, A. (2005). Receptor protein tyrosine phosphatase sigma inhibits axon regrowth in the adult injured CNS. Mol. Cell. Neurosci. *28*, 625–635.
32. Thompson, K.M., Uetani, N., Manitt, C., Elchebly, M., Tremblay, M.L., and Kennedy, T.E. (2003). Receptor protein tyrosine phosphatase sigma inhibits axonal regeneration and the rate of axon extension. Mol. Cell. Neurosci. *23*, 681–692.
33. Fry, E.J., Chagnon, M.J., López-Vales, R., Tremblay, M.L., and David, S. (2010). Corticospinal tract regeneration after spinal cord injury in receptor protein tyrosine phosphatase sigma deficient mice. Glia *58*, 423–433.
34. van der Sar, A., Betist, M., de Fockert, J., Overvoorde, J., Zivković, D., and den Hertog, J. (2001). Expression of receptor protein-tyrosine phosphatase alpha, sigma and LAR during development of the zebrafish embryo. Mech. Dev. *109*, 423–426.
35. van Eekelen, M., Overvoorde, J., van Rooijen, C., and den Hertog, J. (2010). Identification and expression of the family of classical protein-tyrosine phosphatases in zebrafish. PLoS ONE *5*, e12573.
36. Higashijima, S., Hotta, Y., and Okamoto, H. (2000). Visualization of cranial motor neurons in live transgenic zebrafish expressing green fluorescent protein under the control of the islet-1 promoter/enhancer. J. Neurosci. *20*, 206–218.
37. Sagasti, A., Guido, M.R., Raible, D.W., and Schier, A.F. (2005). Repulsive interactions shape the morphologies and functional arrangement of zebrafish peripheral sensory arbors. Curr. Biol. *15*, 804–814.
38. O'Brien, G.S., Rieger, S., Wang, F., Smolen, G.A., Gonzalez, R.E., Buchanan, J., and Sagasti, A. (2012). Coordinate development of skin cells and cutaneous sensory axons in zebrafish. J Comp Neurol. *520*, 816–831.
39. Sun, Q., Schindelholz, B., Knirr, M., Schmid, A., and Zinn, K. (2001). Complex genetic interactions among four receptor tyrosine phosphatases regulate axon guidance in Drosophila. Mol. Cell. Neurosci. *17*, 274–291.
40. Liu, Y., and Halloran, M.C. (2005). Central and peripheral axon branches from one neuron are guided differentially by Semaphorin3D and transient axonal glycoprotein-1. J. Neurosci. *25*, 10556–10563.
41. Streuli, M., Krueger, N.X., Thai, T., Tang, M., and Saito, H. (1990). Distinct functional roles of the two intracellular phosphatase like domains of the receptor-linked protein tyrosine phosphatases LCA and LAR. EMBO J. *9*, 2399–2407.
42. Hofmeyer, K., and Treisman, J.E. (2009). The receptor protein tyrosine phosphatase LAR promotes R7 photoreceptor axon targeting by a phosphatase-independent signaling mechanism. Proc. Natl. Acad. Sci. USA *106*, 19399–19404.
43. Prakash, S., McLendon, H.M., Dubreuil, C.I., Ghose, A., Hwa, J., Dennehy, K.A., Tomalty, K.M., Clark, K.L., Van Vactor, D., and Clandinin, T.R. (2009). Complex interactions amongst N-cadherin, DLAR, and Liprin-alpha regulate Drosophila photoreceptor axon targeting. Dev. Biol. *336*, 10–19.
44. Guan, K.L., and Dixon, J.E. (1991). Evidence for protein-tyrosine-phosphatase catalysis proceeding via a cysteine-phosphate intermediate. J. Biol. Chem. *266*, 17026–17030.
45. Andersen, E.F., Asuri, N.S., and Halloran, M.C. (2011). In vivo imaging of cell behaviors and F-actin reveals LIM-HD transcription factor regulation of peripheral versus central sensory axon development. Neural Develop. *6*, 27.
46. Phan, K.D., Hazen, V.M., Frendo, M., Jia, Z., and Butler, S.J. (2010). The bone morphogenetic protein roof plate chemorepellent regulates the rate of commissural axonal growth. J. Neurosci. *30*, 15430–15440.
47. Raphael, A.R., Perlin, J.R., and Talbot, W.S. (2010). Schwann cells reposition a peripheral nerve to isolate it from postembryonic remodeling of its targets. Development *137*, 3643–3649.
48. Walz, A., McFarlane, S., Brickman, Y.G., Nurcombe, V., Bartlett, P.F., and Holt, C.E. (1997). Essential role of heparan sulfates in axon navigation and targeting in the developing visual system. Development *124*, 2421–2430.
49. O'Brien, G.S., Rieger, S., Martin, S.M., Cavanaugh, A.M., Portera-Cailliau, C., and Sagasti, A. (2009). Two-photon axotomy and time-lapse confocal imaging in live zebrafish embryos. J Vis Exp. *24*, e1129.
50. Kwan, K.M., Fujimoto, E., Grabher, C., Mangum, B.D., Hardy, M.E., Campbell, D.S., Parant, J.M., Yost, H.J., Kanki, J.P., and Chien, C.B. (2007). The Tol2kit: a multisite gateway-based construction kit for Tol2 transposon transgenesis constructs. Dev. Dyn. *236*, 3088–3099.